Ligament Strains Predict Knee Motion After Total Joint Replacement

A Kinematic Analysis of The Sigma Knee

Elvis C.S. Chen[1], Joel L. Lanovaz[2], and Randy E. Ellis[1,2,3]

[1] School of Computing
chene@cs.queensu.ca
[2] Department of Mechanical Engineering
lanovaz@me.queensu.ca
[3] Department of Surgery, Queen's University, Kingston, Ontario, Canada
ellis@cs.queensu.ca

Abstract. A passive forward kinematics knee model was used to predict knee motion of a total joint replacement. Given a joint angle, maps of articular surfaces, and patient-specific ligament properties, this model predicted femorotibial contact locations based on the principle of ligament-strain minimization. The model was validated by physical experiments on a commonly implanted knee prosthesis, showing excellent correspondence between the model and actual physical motion. Results suggest that the knee prosthesis studied required an intact posterior cruciate ligament to induce the desirable roll-back motion, and that a single-bundle model of major knee ligaments generated kinematics similar to that of a multi-bundle ligament model. Implications are that a passive model may predict knee kinematics of a given patient, so it may be possible to optimize the implantation of a prosthesis intraoperatively.

1 Introduction

Total knee replacements (TKRs) are currently designed with noncongruent articular surfaces to accommodate human biomechanics and wear properties of the tibial component [1]. It is known that, when no external forces are present, tensile forces stored in knee ligaments move the knee joint to an equilibrium point where ligament strain is minimized [2].

We have developed and tested a validation protocol for a Forward Knee Kinematics (FKK) model of how human knees move after joint-replacement surgery. A contact-determination algorithm was developed to depict *in situ* femorotibial contact. This algorithm was independently validated using pressure-sensitive film that established the actual femorotibial contact under realistic loading conditions produced by a custom knee jig. The FKK model simulated the physics of the knee jig, which produced a set of *in vivo* femorotibial contact (through the contact determination algorithm) that was compared to *in vitro* contacts predicted by the FKK model. The FKK model was validated; various ligament configurations were considered; and their derived knee kinematics are examined.

J. Duncan and G. Gerig (Eds.): MICCAI 2005, LNCS 3749, pp. 770–777, 2005.

2 Materials and Methods

Articular surfaces of a size-3 Sigma Knee (Johnson & Johnson) were laser-scanned at a resolution of $0.4mm$, resulting in two point clouds of approximately $31,000$ and $19,000$ for each of the femoral and tibial component, respectively. Joint coordinate frames [3] were assigned to these TKR components. The *absolute*, space-fixed coordinate frame was associated with the tibial component, whereas the *relative*, body-fixed coordinate frame was associated with the femoral component. Without lost of generality, the Z-axes were aligned with the anatomical axes of the lower limbs. The X-axes were perpendicular to the Z-axes lying on the sagittal plane with the anterior direction being positive. The Y-axes were derived as the cross product of the two: $Y = Z \times X$.

These two coordinate frames were related by a homogeneous transformation. If $\bar{p}$ is a 3×1 column vector that measures the coordinate of a point in the tibial system, then its corresponding femoral location $\bar{q}$ can be expressed as:

$$\begin{bmatrix} \bar{q} \\ 1 \end{bmatrix} = \begin{bmatrix} R\ \bar{d} \\ 0\ 1 \end{bmatrix} \begin{bmatrix} \bar{p} \\ 1 \end{bmatrix} \tag{1}$$

where R is a 3×3 orthogonal rotational matrix and $\bar{d}$ is a 3×1 displacement vector. Because the tibia was assumed to be fixed, R and $\bar{d}$ represented the relative joint angle and position of the femoral component. The rigid-body transformation of a point is a rotation (R) to the mobile coordinate frame followed by a linear displacement ($\bar{d}$).

2.1 Forward Knee Kinematics

The passive forward kinematics knee model proposed by Chen *et. al.* [2] was implemented with a minor modification. The strain energy for each ligament was calculated as

$$E = \begin{cases} .5 \times K \times (L - \tilde{L})^2 + B \times (L - \tilde{L}), & \text{if } L \geq \tilde{L} \\ 0, & \text{if } L < \tilde{L} \end{cases} \tag{2}$$

where $\tilde{L}$ was the neutral length of the ligament, L was the Euclidean distance between ligament attachment points, and K and B were the spring constants.

2.2 Contact Determination Algorithm

Mathematically, two points are in contact if they coincide in space and have point normals opposite in direction. Let $\bar{p}$ and $\bar{q}$ be contacting points on the femoral and tibial components, respectively, with associated normals $\bar{p_n}$ and $\bar{q_n}$ being

$$\| p - q \| \leq \delta \tag{3}$$

$$-(p_n \cdot q_n) \geq 1 - \epsilon \tag{4}$$

where $\| \bullet \|$ denotes the Euclidean vector norm, and δ and ϵ are distance and angular tolerances, respectively. These tolerance are necessary because the articular surfaces were sampled at a finite resolution. Equation (3) and (4) were the *contact conditions* used to determine points on the contacting surfaces.

To validate the contact determination algorithm, a static contact analysis experiment was performed using a commercial 4-DOF knee implant wear test machine (Force 5, Advanced Mechanical Technologies Inc., USA). The femoral and tibial components were mounted on custom jigs using a polymethylmethacrylate cement that is typically used to affix knee prostheses to human bone. Dynamic Reference Bodies (DRBs) were rigidly fixed to the femoral and tibial components. An accurate optical system (Optotrak 3020, Northern Digital, Canada) was used to record the 6D poses. Registration between the DRBs and the component models were obtained using the Iterative Closest Point [4] algorithm.

For the static trials, the neutral (0° flexion) pose of the components was found using the guidelines given in ISO Standard 14243-3. This standard was used for TKR wear testing and supplies four control waveforms (vertical force, flexion angle, anterior/posterior position and internal/external rotation) for a typical walking cycle. Six poses corresponding to 0, 13, 45, 56, 72,and 88 percent of the standard walking cycle were chosen for testing. These corresponded to start, 1^{st} max vertical force, 2^{nd} max vertical force, max AP position, max FE angle and max IE angle.

For each test pose, a Fuji Prescale pressure sensitive film (Ultra Super Low Pressure Grade), cut to fit the tibial contact surfaces, was fixed to the tibial component using two-sided tape on the anterior region of the component (where femorotibial contact was not possible). A small vertical load was applied to the tibia to bring the components into initial contact with minimal sliding. The 6D pose for each component was collected and was used in the contact-determination algorithm.

After the components were unloaded, a tracked optical probe was used to trace the outline of the Fuji film stains while the film was still in place on the tibial surface. The 3D locations of traced points were superimposed on the contact regions determined by the contact determination algorithm, depicted in Fig. 1.

2.3 Spring Ligament Apparatus

To validate the FKK model, a physical apparatus was constructed to simulate passive knee flexion after TKR. The femoral component was mounted on a rigid frame and rotated so that the femoral long axis was perpendicular to gravitation. Plexiglas plates were rigidly attached to the apparatus frame approximately $3cm$ from the medial and lateral sides of the femoral component. The tibial component was mounted on the proximal end of a simulated shank (i.e., the distal lower limb segment). The shank consisted of four long threaded rods, arranged to form a $6cm \times 6cm \times 30cm$ parallelepiped shape and held in place by Plexiglas end plates. A $2.2kg$ mass was fixed at the distal end of the shank, approximating the inertia of the median North American foot.

A DRB was rigidly fixed to the femoral mounting jig and a second DRB was rigidly attached to the shank. The component models were registered to the kinematic system with the same procedure used in the static contact experiments.

Steel tension springs were used to simulate some of the ligament constraints of the knee joint. The ends of each ligament spring were fixed to spherical rod-end bearings. The spherical bearings for each ligament spring were then fixed on one end to Plexiglas plates beside the femur and on the other end to custom ABS jigs attached to the shank segment. The apparatus was designed to allow for one, two, or three springs to

be attached on each of the medial and lateral sides of the joint and at various positions along the proximal/distal axis of the shank. This simulated the ligament constraints of the MCL and LCL.

Two sets of experiments were conducted with this apparatus. The first one involved a total of 6 springs, 3 simulating the MCL and 3 simulating the LCL. The second experiment involved only 2 springs, 1 simulating the MCL with the other simulating the LCL. The mechanical properties of the springs are listed in Table 1. In both experiments, the springs were positioned symmetrically with respect to the medial and lateral sides. The exact physical insertion locations for the springs, relative to the component models, were obtained using the calibrated optical tracking probe.

Table 1. The mechanical properties of steel tension springs used in Eqn. 2

	MCL 1	MCL 2	MCL 3	LCL 1	LCL 2	LCL 3	MCL	LCL
unloaded length (mm)	65.0	65.0	65.0	65.0	65.0	65.0	124.0	125.0
K (N/mm)	.66	.66	.65	.66	.66	.66	1.36	1.37
B (N)	5.90	5.80	6.00	6.80	4.00	6.50	2.57	5.53

The goal of the experimental setup was to simulate passive joint flexion. The simulated joint was extended manually in discrete increments from approximately 100° of flexion to 0° of flexion and then flexed back to 100° of flexion. A total of 171 and 36 poses were obtained with 6 and 2 springs respectively. At each pose, the joint was allowed to rest to a stable configuration with minimal force applied to the shank.

2.4 Patient-Specific Kinematics

It was technically difficult to include a PCL mechanism in our apparatus. Instead, we generated a physiologically plausible knee kinematics by adapting the patient-specific ligament data of Chen *et. al.* [2]. A total of 11 ligament bundles were taken into consideration: 3, 4, and 4 for each of the PCL/MCL/LCL, respectively. The MCL was symmetrical to the LCL.

Four simulations were performed. The first simulation utilized all 11 ligament bundles. The second simulation considered the knee kinematics without the PCL. The 3^{rd} and the 4^{th} simulations were the same as the first two, but with single-bundle ligaments in place of the detailed bundles. The single-bundle ligament was artificially generated by taking the geometrical mean of the ligament insertions in the multi-bundle ligament configuration, using summed spring constants.

3 Results

3.1 Contact Determination Algorithm

Figure 1 depicts a typical experimental result between the Fuji film produced with the Force 5 knee tester and the contact determination algorithm (with $\delta = 0.4mm$ and $\epsilon = 0.004$). The peripheries of the Fuji contacts were digitized and superimposed to the region produced by the algorithm. They show high degree of agreement.

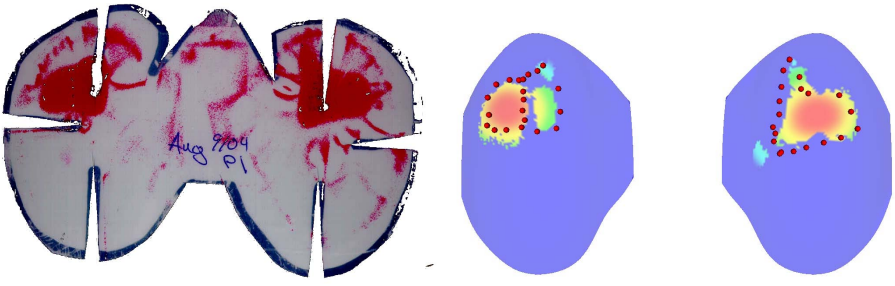

Fig. 1. Contacts determined using Fuji film and the contact determination algorithm

3.2 Apparatus Kinematics

For each recorded joint pose, two types of contact locations were generated. First, the *in situ* contact locations were determined using the contact determination algorithm. The same joint angle was used in the FKK model and, in conjunction with spring information, the *in vitro* contact locations were calculated. Figure 2 depicts a typical result: for the given joint angle, an *energy map* was produced depicting all feasible contact locations (Fig. 2(a)). The subset of the feasible contacts resulting in the minimal ligament strain energy formed the *in vitro contact patch* (Fig. 2(b)). The *instantaneous contact points* were calculated as the point on articular surfaces closest to the centroid of the contact patch, and they constrained the amount of the femoral component displacement ($\bar{d}$ in (1)).

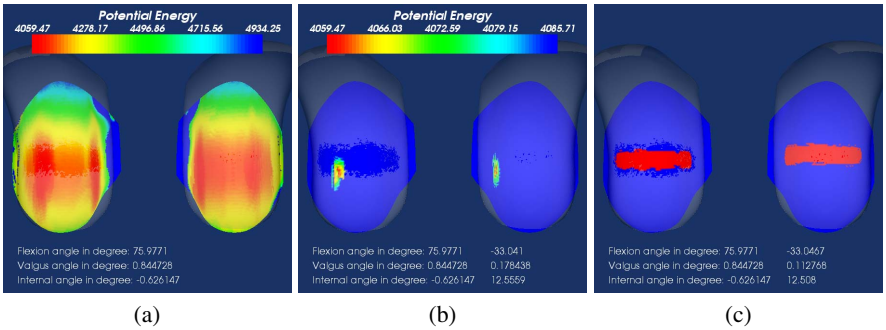

(a) (b) (c)

Fig. 2. Contact predicted by the FKK model and the contact determination algorithm

For experiments involving 6 springs, the difference in the displacement vector $\bar{d}$ calculated by the two methods were on average $0.43mm$, with a standard deviation of $0.35mm$. For experiments involving 2 springs, the mean difference was $0.69mm$ with a standard deviation of $0.15mm$.

3.3 Sigma Knee Kinematics

To analyze the kinematics generated by the mechanical springs, contact locations from $0°$ to $120°$ flexion were calculated at $1°$ increments using the FKK model. Figure 3 depicts the contact locations generated using the 6-spring and 2-spring configurations. The placement of contact locations suggest that the kinematics for both spring configuration were basically the same, and that the femoral component spun in place throughout flexion with no obvious anterior-posterior translation. To further demonstrate the difference in kinematics generated, Fig. 4(a) depicts the femoral translation through flexion angle and Fig. 4(b) depicts the Euclidian distance in the displacement vectors $\bar{d}$ for each spring configuration. mean difference was $0.62mm$ with a standard deviation of $0.36mm$, which is negligible.

Four simulations were generated with the physiologically plausible ligament configurations. Contact locations were calculated from $0°$ to $120°$ flexion at $1°$ increments (Fig. 5). The amount of ligament strain stored in knee ligament are depicted in Fig. 5.

In simulations accounting for a PCL mechanism, contact locations at full extension were located at the anterior portion of the tibia; for these, the MCL and LCL were both taut and the PCL was relaxed. As the knee flexed, the contact locations gradually moved posteriorly as the PCL tightened. At full flexion, the MCL and LCL were relaxed but the PCL was taut, pulling the femur posteriorly. In all cases, at the beginning and the end of flexion there were some spinning motion.

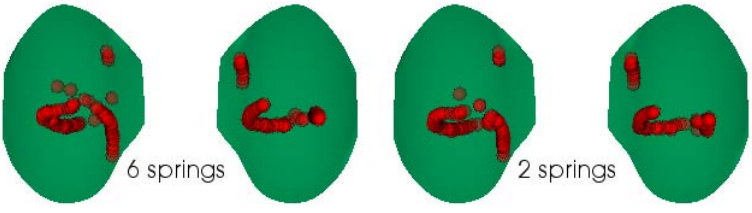

Fig. 3. Contact locations for the 6-springs (a) and 2-springs (b) knee jig from full extension to $120°$ flexion. In both configurations, the femoral component spun in place through the flexion.

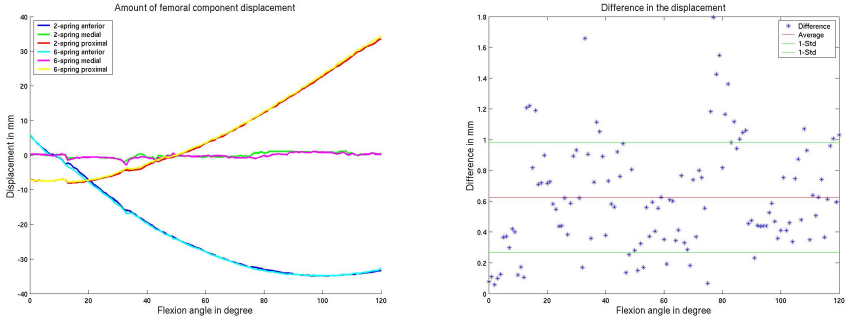

Fig. 4. Plot of the femoral displacement determined with 6-spring and 2-spring knee jig

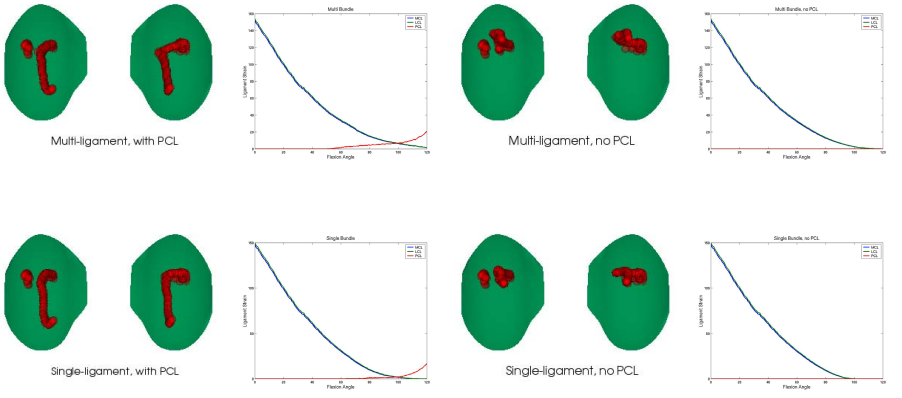

Fig. 5. Contact paths and ligament profile of different ligament configurations: (a) multi-bundle ligament, (b) multi-bundle without PCL, (c) single-bundle ligament, (d) single-bundle without PCL

4 Discussion

The contact determination algorithm was based on (3) and (4). The querying mechanism was implemented with a KD-tree [5] for a speedy retrieval. On a 2GHz PC, the plots depicted in Fig. 1 were generated in less than 1 second, which is acceptable for intraoperative use. This algorithm was validated by a Fuji film study, which is widely accepted as the gold standard for knee kinematics [6].

A custom apparatus was constructed and used to further validate the passive forward kinematics knee model. Two physical experiments involving different ligament configurations were conducted. In each case, the contact locations predicted by the FKK model agreed with the gold-standard *in vitro* contact locations determined with the apparatus with sub-millimeter accuracy.

After the FKK model was validated, various physiologically plausible ligament configurations were used to analyze the kinematics of a specific prosthesis (the Sigma Knee). In simulations without a PCL, the contact locations for all flexion angles were located in the anterior portion of the tibia. This implied that the femur was basically spinning in place, exactly as was observed in the apparatus with mechanical springs. With a PCL present, the contact location gradually moved posteriorly as the knee flexed. In all simulations, there was no obvious difference in the kinematics generated with a multi-bundle ligament model versus a single-bundle ligament model.

5 Conclusion

To determine the *in situ* femorotibial contact location, a fast contact-determination algorithm was developed and validated with the gold-standard pressure-sensitive Fuji film. Physical experiments demonstrated that the Forward Kinematics Knee (FKK) model [2] predicted knee motion with sub-millimeter accuracy.

After the FKK model was validated, various ligament configurations were used to determine their influence on the predicted knee kinematics. Simulation results suggested that:

- The Sigma Knee requires a PCL mechanism to produce a roll-back motion;
- In the absence of a PCL mechanism, the Sigma Knee spins in place; and
- In both simulated and experimental results, multi-fiber and single-fiber ligament configuration produced similar kinematics.

This study is limited by the number of ligaments examined, the configurations of the ligaments, and that only one prosthesis was simulated. Further enquiry into this subject is indicated.

These results have implications for both knee modelers and for surgeons. For knee modelers, the results suggest that a good simple model of knee ligaments suffice to model the Sigma Knee, so it is better to get a good rough guess of knee-ligament geometry rather than to toil for a detailed model. For surgeons, these results suggest that the high surface conformity of the Sigma Knee bearing surfaces are relatively insensitive to implantation geometry, that is, that the minor variations of surgical implantation are not likely to produce major changes in kinematics. Our results suggest that the Sigma Knee, in the hands of an experienced surgeon, may produce motion consistent with a normal healthy knee.

References

1. O'Connor, J.J., Goodfellow, J.W.: The role of meniscal bearing vs. fixed interface in unicondylar and bicondylar arthroplasty. In Goldberg, V.M., ed.: Controversis of Total Knee Arthroplasty. Raven Press (1991) 27–49
2. Chen, E., Ellis, R.E., Bryant, J.T., Rudan, J.F.: A computational model of postoperative knee kinematics. Medical Image Analysis **5** (2001) 317–330
3. Grood, E.S., Suntay, W.J.: A joint coordinate system for the clinical description of three-dimensional motions: application to the knee. Journal of Biomechanical Engineering **105** (1983) 136–144
4. Besl, P.J., McKay, N.D.: A method for registration of 3-D shapes. IEEE Transactions on Pattern Analysis and Machine Intelligence **14** (1992) 239–256
5. Bentley, J.L.: Multidimensional binary search trees used for associative searching. Communication of the ACM **18** (1975) 509–517
6. Zdero, R., Fenton, P.V., Rudan, J., Bryant, J.T.: Fuji film and ultrasound measurement of total knee arthroplasty contact areas. The Journal of Arthroplasty **16** (2001) 367–375